International Journal of Pharmaceutics 431 (2012) 190–196

Contents lists available at SciVerse ScienceDirect

International Journal of Pharmaceutics

journal homepage: www.elsevier.com/locate/ijpharm

Pharmaceutical Nanotechnology

Enhanced antitumor efficacy of cisplatin by tirapazamine–transferrin conjugate

Lin Wu[a,b,1], Jinhui Wu[a,*,1], Yuanyuan Zhou[a], Xiaolei Tang[a], Yanan Du[c], Yiqiao Hu[a,**]

[a] State Key Laboratory of Pharmaceutical Biotechnology, Nanjing University, 22 Hankou Road, Nanjing 210093, China
[b] First Affiliated Hospital of Nanjing Medical University, Nanjing 210029, China
[c] Department of Biomedical Engineering, School of Medicine, Tsinghua University, Beijing 100084, China

ARTICLE INFO

Article history:
Received 11 December 2011
Received in revised form 31 March 2012
Accepted 9 April 2012
Available online 15 April 2012

Keywords:
Transferrin
Tirapazamine
Cisplatin
Targeting anti-tumor effect
Tissue distribution

ABSTRACT

Combination of tirapazamine (TPZ) with cisplatin has been studied extensively in clinical trial for tumor therapy. However, in phase III clinical trial, the combination therapy did not show overall survival improvement in patients. To decrease the side effects and increase the efficacy of the combination therapy, TPZ was conjugated with transferrin (Tf-G-TPZ) for targeted delivery and co-administered with cisplatin. In vitro toxicity study showed that the combination of Tf-G-TPZ with cisplatin induced substantially higher cytotoxicity of tumor cells than the combination of TPZ and cisplatin. After Tf-G-TPZ was intravenously injected into tumor-bearing mice, its total accumulation in tumor was 2.3 fold higher than that of the unmodified TPZ, suggesting transferrin-mediated target delivery of TPZ into the tumor tissue. With the increased accumulation of Tf-G-TPZ in tumor, the synergistic anti-tumor effects of Tf-G-TPZ and cisplatin were also enhanced as showed by the 53% tumor inhibition rate. Meanwhile, the side effects such as body weight lost were not significantly increased. Therefore, Tf-G-TPZ holds great promise to a better substitute for TPZ in the combination therapy with cisplatin.

1. Introduction

Cisplatin is one of the most widely used chemical compounds in antitumor chemotherapy (Fruscio et al., 2011; Yamasaki et al., 2011; Ying et al., 2011). It was first synthesized by Mickäel Peyrone in 1844, however its antitumor activity was not discovered until 1960s (Rosenberg et al., 1965). In 1971, cisplatin was introduced into clinical trials and approved by FDA in 1979 for the anti-cancer therapies of ovarian, testis and head and neck cancers (Todd and Lippard, 2009). When exposed to cancer cells, the chloride ligands within cisplatin are slowly displaced by water, allowing the platinum atom to bind to the intracellular DNA bases resulting in the formation of several types of chemical bonds. The most abundant bonds are the intrastrand crosslinks between two adjacent DNA bases, which induce cell apoptosis and death (Crul et al., 2002). In clinic, cisplatin has been intravenously administered for treatment of solid malignancies (Dickson et al., 2011; Moriyama-Gonda et al., 2008). However, cisplatin-resistant disease always occurs during the treatment. The resistance of tumors to cisplatin might be attributed to the reduction in cellular uptake, the increased detoxification and the increased DNA repair of the cancer cells (Koberle et al., 2010; Stordal and Davey, 2007).

Tirapazamine (TPZ), a lead bioreductive agent, has been shown to potentiate the antitumor efficacy of cisplatin (Marcu and Olver, 2006). Under hypoxic conditions, TPZ is bioreduced to a nitroxide-base free radical that abstracts hydrogen from DNA strands, thereby causing breaks in DNA (Reddy and Williamson, 2009). Incubation of cancer cells with TPZ under hypoxia conditions prior to cisplatin treatment inhibited the self-repair of the DNA damage induced by cisplatin, thus enhancing its antitumor efficacy (Kovacs et al., 1999). The combination therapy of TPZ with cisplatin has also been extensively evaluated in clinical trial for cancer treatment. However, it did not improve overall survival in patients with advanced head and neck cancer in phase III clinical trial (Rischin et al., 2010). Furthermore, incorporation of TPZ to cisplatin treatment leads to a significant increase in unwanted toxicities which causes severe adverse effects including nausea, vomiting, myalgia, diarrhea and muscle spasms (Adam et al., 2006; Covens et al., 2006). The unwanted toxicity might be produced by the enhanced non-specific DNA crosslink to both the normal and cancer cells when TPZ is co-administered with cisplatin. Therefore, targeted delivery and treatment can improve the therapeutic efficacy of the combination treatment by reducing the adverse effect and increasing the overall survival in patients.

Transferrin, an 80 kDa glycoprotein, has been widely applied as a targeted drug delivery carrier (Amet et al., 2010; Hong et al., 2010; Park, 2010). It naturally functions as iron supply to cells in the process of DNA synthesis (Jensen et al., 2011; Wang et al., 2011). Transferrin has high affinity for transferrin receptor which

* Corresponding author. Tel.: +86 13913026062; fax: +86 25 83596143.
** Corresponding author. Tel.: +86 13601402829; fax: +86 25 83596143.
E-mail addresses: wuj@nju.edu.cn (J. Wu), huyiqiao@nju.edu.cn (Y. Hu).
[1] Lin Wu and Jinhui Wu contributed equally to this work.

0378-5173/$ – see front matter © 2012 Elsevier B.V. All rights reserved.
http://dx.doi.org/10.1016/j.ijpharm.2012.04.032

mediates its internalization into endosomal acidic compartments via endocytosis. The expression of transferrin receptors is particularly prevalent on rapidly dividing cells such as tumor cells, which makes transferrin an ideal drug carrier for targeted anti-tumor therapy. Transferrin as drug carrier has been studied extensively and transferrin conjugated with a modified diphtheria toxin, named TransMID, has been shown to be effective in treating patients suffering from inoperable, recurrent high grade gliomas (Rainov and Soling, 2006).

The main aim of this study is to evaluate whether human serum transferrin can mediate the targeted delivery of TPZ to tumor and achieve a higher anti-tumor efficacy when co-administered with cisplatin. Transferrin–tirapazamine (Tf-G-TPZ) conjugate was synthesized by traditional bifunctional crosslinking method. A full characterization demonstrated TPZ was successfully conjugated with transferrin as the ratio of 6:1. Via transferrin mediated delivery, the concentration of Tf-G-TPZ in tumor tissue could be significantly increased and hence the antitumor effect of Tf-G-TPZ was enhanced when co-administrated with cisplatin.

2. Material and methods

2.1. Material

Transferrin used in the synthesis process was purified in our lab. More details about the purification and characterization of transferrin can be found in our previous publication (Wu et al., 2008). Porcine serum was obtained from HyClone Bio-Engineering Co., Ltd. (Lanzhou, China). TPZ was obtained from Shunlong Chemical Co., Ltd. (Shangyu, China). Glutaric anhydride, NHS (hydroxysuccinimide) and EDC (1-ethyl-3-(3-dimethylaminopropyl) carbodiimide) were purchased from Medpep Co., Ltd. (Shanghai, China). The BCA (bicinchoninic acid) protein assay kit was purchased from Kengentec Co., Ltd. (Nanjing, China). Cell culture media (DMEM, Dulbecco's modified Eagle's medium) was obtained from Invitrogen (CA, USA) and fetal calf serum (FCS) was purchased from National HyClone Bio-Engineering Co., Ltd. (Lanzhou, China). All culture flasks were obtained from Corning (USA).

2.2. Synthesis of Tf-G-TPZ

Tf-G-TPZ was prepared according to the method of Kato et al. (1983). Briefly, TPZ was first reacted with glutaric anhydride to form N-glutaryl-TPZ. Then 14.6 mg N-glutaryl-TPZ, 10 mg EDC and 6 mg NHS were dissolved in 2 ml DMF (N,N-dimethylformamide) and mixed well by a vertical mixer for 4 h. After 12 h incubation at 4 °C in the dark, the suspension was centrifuged and the supernatant was collected. Then 133 mg Tf dissolved in 5 ml carbonate buffer (0.05 M, pH 9.6) was added into the supernatant. A little amount of insoluble material was formed and removed by centrifugation, and the supernatant was concentrated to approximately 2.0 ml by centrifugation at 4 °C and 4000 rpm with CENTRIPREP-10-concentrators (Millipore, MA, USA) (Beyer et al., 1998). The concentrated sample was subjected to gel filtration on a Sephadex G-25 column (2.0 cm × 20 cm) with 0.02 M phosphate buffer to get rid of the unreacted TPZ derivative. The macromolecular fractions containing Tf-G-TPZ were collected, dialyzed against distilled water and lyophilized.

2.3. Characterization of Tf-G-TPZ

Total protein concentration of the purified Tf-G-TPZ was determined using a bicinchoninic acid (BCA) protein assay kit. A stock solution (C_{TPZ} = 300 μM) of Tf-G-TPZ was subsequently employed in all of the characteristic experiments. The characteristic absorption peak of conjugate was determined using a UV-visible spectrophotometer (SHIMADZU, Japan).

The purity of Tf-G-TPZ was determined at 254 nm with an analytical HPLC-Gel-Filtration column (Bio-Gel® SEC 50-XL, 300 mm × 7.8 mm) from Bio-Rad (mobile phase: 0.15 M NaCl, 0.01 M NaH_2PO_4, 5% CH_3CN, pH 7.0) (Kratz et al., 1998). The integrity and aggregation of Tf-G-TPZ were evaluated by SDS-PAGE, using 12% polyacrylamide gel with 2-mercaptoethanol. After electrophoresis, the gel was stained with Coomassie Blue R-250 and destained in 45:10:45 (methanol:glacial acetic acid:water).

Matrix-assisted laser desorption ionization (MALDI) mass spectrometry with time-of-fight (TOF) was performed using an ultraflex II TOF/TOF instrument (Bruker-Daltonics, Germany) equipped with a smart beam laser operating at 200 Hz. A saturated solution of 2,5-dihydroxybenzoic acid (DHB) in 30% acetonitrile and 0.1% trifluoroacetic acid was prepared as a matrix solution. An aliquot (1 μl) of the sample solution was mixed with an equal aliquot of the matrix solution, and 1 μl of the matrix solution was spotted onto the target plate and evaporated under a gentle stream of warm air. Mass spectra were acquired in positive ion reflector mode using a reflectron voltage of 25000 V, accelerating voltage at 92.8%, lens voltage at 26% and pulsed ion extraction of 150 ns. External calibration was performed for molecular assignments using a standard of bovine serum albumin with $[M+]^+$ at 66.5 kDa.

2.4. Release profile of Tf-G-TPZ

Tf-G-TPZ was dissolved in 0.02 M phosphate buffer (pH 7.4 and 6.5) or 0.02 M acetate buffer (pH 5.2 and 4.0) both containing 0.15 M NaCl and 0.02% sodium azide in a total volume of 2 ml to give a final concentration of 5 mg/ml. Then the sample solution was put into a dialysis bag. Each bag was placed into capped, wide-mouth jars containing 50 ml of the appropriate release medium incubated at 37 °C. For each trial with Tf-G-TPZ, a corresponding trial with un-conjugated TPZ and a physical mixture of transferrin/TPZ were conducted as controls. After varying periods of incubation (0, 1, 2, 3, 4, 5, 7, 9, 11, 13, 24, 28, 32, 36, 48 h), 1 ml of release medium was withdrawn and replaced with fresh medium to maintain a constant volume (Ofner et al., 2006). Samples removed at intervals were immediately frozen. All samples were collected and analyzed by HPLC. The HPLC analysis for TPZ was performed on a Symmetry® C18 column (5 μm, 250 mm × 4.6 mm) and recorded at 254 nm. The mobile phase was 14% (v/v) acetonitrile containing 0.1% acetic acid.

2.5. Cell culture

The SW1116 (Human Colorectal adenocarcinoma cells) were purchased from Kengentec Co., Ltd. (Nanjing, China). Cells were maintained as monolayer cultures in RPMI 1640 culture medium with 10% (v/v) heat-inactivated FCS (Fetal calf serum), 2 mM glutamine, and 0.1 mg/ml of penicillin/streptomycin. Cells were cultured in a humidified incubator at 37 °C and 5% CO_2. Medium was routinely changed every 3 days.

2.6. In vitro cytotoxicity

100 μl cell suspensions were seeded in 96-well flat-bottomed microtiter plate at a density of 1×10^5 cells/ml. After pre-incubating for 12 h, medium was removed by aspiration and replaced by TPZ (50–400 μM), Tf-G-TPZ (12.5–100 μM) or Cisplatin (20 μM). After 48 h culture at 37 °C, cells were stained by 10 μl MTT (3-(4,5)-dimethylthiazol-2-yl)-2,5-diphenyltetrazolium bromide, 5 mg/ml in PBS) and re-incubated for an additional 3 h. Subsequently, the

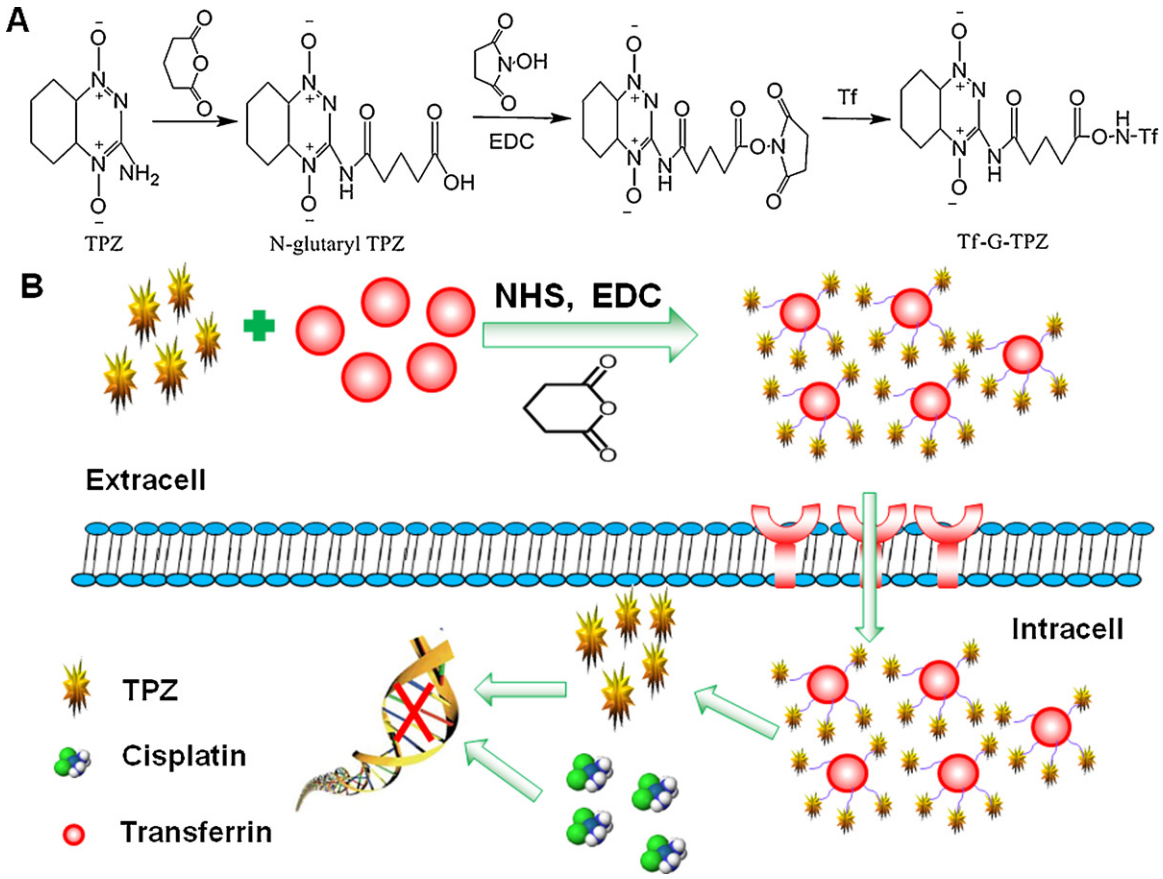

Fig. 1. (A) TPZ was modified with carboxyl groups by reacting with glutaric anhydride. The modified carboxyl was activated with NHS and formed an active ester group in the presence of EDC. Then the free amino on transferrin was crosslinked with the modified TPZ and formed Tf-G-TPZ. (B) The combinatorial effects of Tf-G-TPZ and cisplatin. Tf-G-TPZ was delivered into the tumor cells by endocytosis mediated by transferrin receptors overexpressed on the tumor cell surface. Due to the decrease in pH, TPZ was released into the cytoplasm from Tf-G-TPZ. Cisplatin could inhibit the formation of DNA intrastrand and interstrand adducts, while TPZ could inhibit the repair of cisplatin-induced interstrand adducts and thus an increased antitumor effect could be achieved.

supernatant was discarded and 150 μl DMSO was added to dissolve the formed formazan crystals. The absorption was measured at 570 nm using a microplate reader. IC_{50} values (50% inhibitory concentration) were calculated by Origin 8.0 software.

2.7. Biodistribution in mouse sarcoma S180 cell tumor bearing mice

Male Kunming strain mice (KM, 18–22 g) were purchased from Qinglongshan, Experimental Animal Center (Nanjing, China). Animal care, experiments and protocols were approved by the Nanjing University Animal Care and Use Committee. Mouse sarcoma 180 (S180) cells were purchased from the Institute of Biochemistry and Cell Biology, Shanghai Institutes for Biological Sciences, Chinese Academy of Sciences (Shanghai, China).

Mice were injected subcutaneously in the right armpit with S180 cells (10^7) suspended in normal saline (Liu et al., 2012; Qin et al., 2002). Tumor volume was permitted to reach 1 cm^3 (around 10 days) and only those mice bearing regular round shape tumor were selected in this study. TPZ or Tf-G-TPZ was intravenously injected into the tail vein at the dose of 20 mg/kg. Mice were sacrificed after defined time periods (10 min, 1 h, 2 h and 4 h). Heart, liver, spleen, lung, kidney and tumor tissues were collected and 0.1 g wet tissue was weighed. 1 ml normal saline was added to the wet tissue and homogenized for 5 min. The samples (400 μl) were transferred to a 1.5 ml Eppendorf tube and mixed with 800 μl methanol. The mixture was vortexed well and then centrifuged for 10 min at 15,000 rpm. The supernatant was injected to HPLC for analysis (Siim et al., 2004).

2.8. Anti-tumor efficacy and toxicity combined with cisplatin

Treatment was initiated when the tumor diameter reached about 0.5 cm (around 7 days). Mice were randomly divided into six groups ($n = 9$ or 10). TPZ and Tf-G-TPZ were administered at a dose of 20 mg/kg either alone or combined with cisplatin, which was administered 2 h later at a dose of 1 mg/kg. The control group received corresponding amounts of saline. In addition, a group treated with cisplatin alone was also included. Cisplatin was injected intraperitoneally (Abuzeid et al., 2009; Tikoo et al., 2009). Other drugs were injected intravenously. The overall treatment time was 8 days. Drugs were administered once a day for all 8 days. Tumor size was monitored daily by measuring subcutaneous tumor grafts (major and minor axis) with a caliper. In addition, animal weight was measured daily for systemic toxicity assessment. Tumor volumes were calculated using the formula: $a^2 \times b \times 0.52$ (where a is the shortest and b is the longest diameter) (Wu et al., 2009).

2.9. Statistics

Results were expressed as mean ± standard deviation. Statistical significance of differences was assessed using an ANOVA test

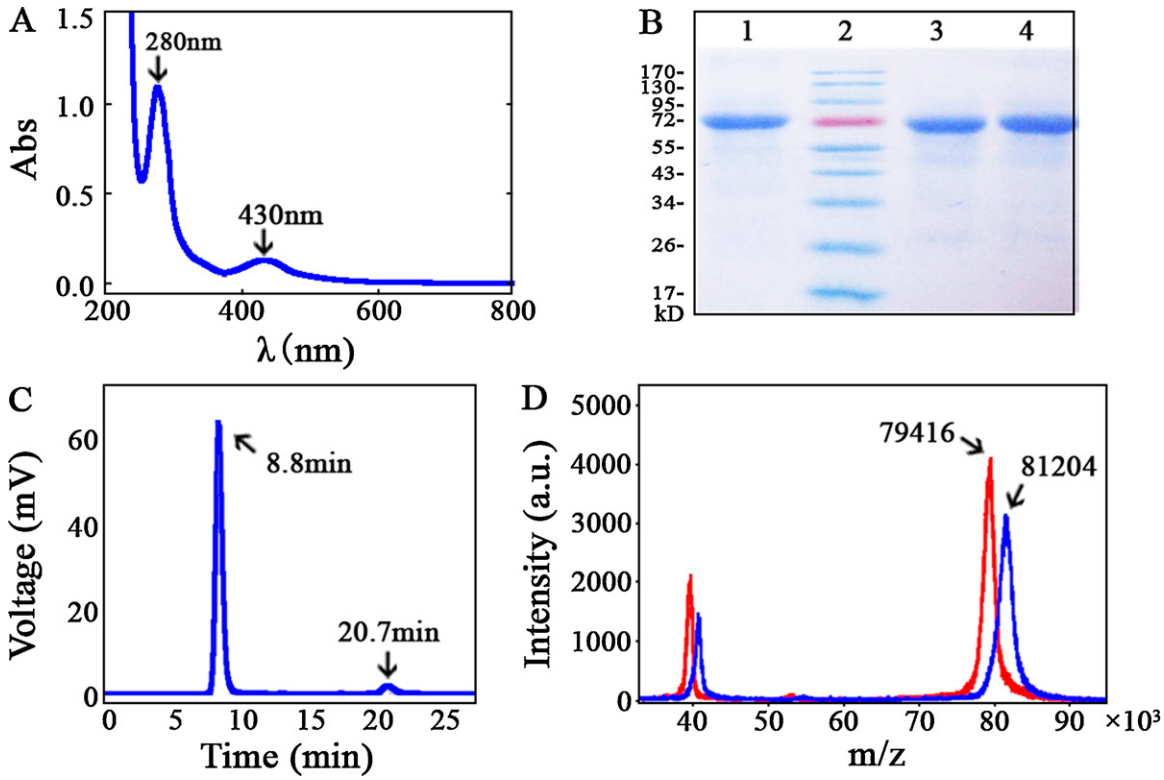

Fig. 2. Characterization of Tf-G-TPZ. (A) UV absorbance profiles of Tf-G-TPZ. (B) SDS-PAGE gel electrophoresis of Tf-G-TPZ. Lanes 1–4 were Tf-G-TPZ, protein marker, Tf from sigma and Tf purified in house, respectively. Results indicated Tf-G-TPZ was mostly in the monomer form. (C) Size-exclusion HPLC chromatogram of Tf-G-TPZ conjugate showed that Tf-G-TPZ had a high purification. (D) MALDI-TOF MS of Tf and Tf-G-TPZ. The increase in the molecular weight (from 79416 to 81204) was due to the TPZ modification on Tf.

and Student's *t*-test. A *p*-value of less than 0.05 was considered significant.

3. Results and discussion

3.1. Synthesis and characterization of Tf-G-TPZ

Transferrin–tirapazamine (Tf-G-TPZ) conjugate was synthesized by traditional bifunctional crosslinking method (Fig. 1). First, TPZ was modified with carboxyl group by reacting with glutaric anhydride. The modified carboxyl could be activated with hydroxysuccinimide (NHS) and formed an active ester group in the presence of 1-ethyl-3-(3-dimethylaminopropyl) carbodiimide (EDC). Then the free amine groups on transferrin would crosslink with the activated TPZ to form Tf-G-TPZ.

To characterize the synthesized conjugate, HPLC analysis, bicinchoninic acid assay and UV scanning were performed. The ratio of TPZ to Tf in various lots was about 4.8:1–5.4:1 with an average conjugation number of 5.1. The ultraviolet absorption spectrum of Tf-G-TPZ showed two typical peaks at 430 nm and 280 nm, corresponding to TPZ and Tf, respectively (Fig. 2A). While unmodified TPZ showed a typical peak at 465 nm, the blue shift of the typical peak in the TPZ-G-Tf conjugate was due to the formation of N-glutaryl-TPZ.

Although the synthesis process was mild, protein aggregation or degradation may still occur. Therefore, SDS-PAGE was used to evaluate the integrity of the synthesized Tf-G-TPZ conjugate. The single band corresponding to Tf-G-TPZ was observed in SDS-PAGE (Fig. 2B), suggesting the conjugate was mostly synthesized as monomer.

To determine the purity of the synthesized conjugate, Tf-G-TPZ was injected into a typical HPLC Size Exclusion chromatogram. The absorption wavelength of 254 nm was chosen for determining TPZ concentration (Fig. 2C). The main peak at 8.8 min was corresponding to Tf-G-TPZ, while TPZ was eluted at 20.7 min. Tf-G-TPZ contained less than 2% TPZ, suggesting high purity of the synthesized Tf-G-TPZ.

MALDI-TOF mass spectrometry analysis showed a typical increase (1788 Da) in the molecular weight of Tf as a result of TPZ conjugation (Fig. 2D). The increased molecular weight of Tf-G-TPZ implied that about six TPZ molecules (Mw = 292) were conjugated to one Tf molecule. The result was consistent with the ratio calculated by the spectroscopy mentioned in the above section. Meanwhile, in the mass spectra, both Tf and Tf-G-TPZ showed a major peak with high intensity, suggesting high purity of the synthesized product qualified for following experiments.

3.2. Release profile of Tf-G-TPZ

The effects of pH on the release profile of Tf-G-TPZ conjugate were evaluated (Fig. 3). Four different pH values (4.0, 5.2, 6.5 and 7.4) were tested. In pH 7.4 medium, approximately 22% of TPZ was released from the conjugate after 48 h. While in pH 4.0 medium, about 60% of TPZ was released, which was about 2.7 fold faster than pH 7.4 With the decrease of pH, the percentage of released TPZ was increased, indicating that the conjugate is acid-sensitive. While in control group such as un-conjugated TPZ and a physical mixture of transferrin/TPZ, 100% of TPZ were released in 1 h (data not shown).

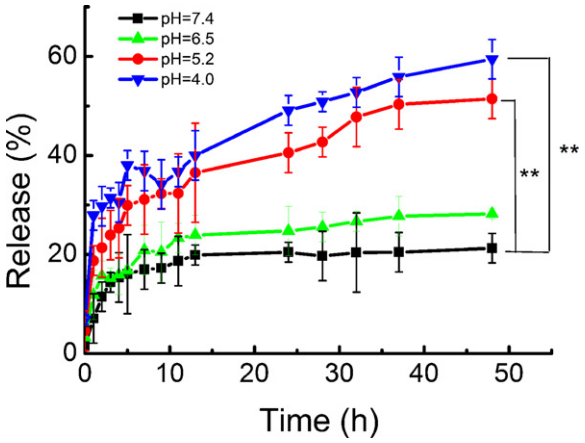

Fig. 3. Effect of pH on the release of TPZ from Tf-G-TPZ. The pH sensitivity of Tf-G-TPZ was studied at pH values of 4.0, 5.2, 6.5 and 7.4 over a period of 48 h. Sample solutions were incubated at 37 °C with 100 rpm shaking. $^{**}p < 0.01$, significantly different from pH 7.4 ($n = 3$).

The acid-sensitive property of Tf-G-TPZ made the release only occur in acid environment. When injected in vivo, Tf-G-TPZ was internalized into the endosomal acidic compartments of tumor cells via receptor endocytosis mediated by transferrin receptor expressed on tumor cell surface. Due to the acid-sensitive property, TPZ was released from transferrin which induced DNA strand breakage to kill tumor cells.

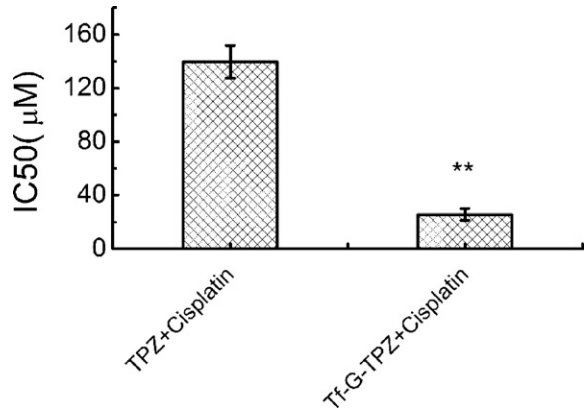

Fig. 4. Combinatorial effects of Tf-G-TPZ and cisplatin in SW1116 cell line. TF-G-TPZ plus cisplatin showed a significant decrease in IC_{50} ($^{**}p < 0.01$, $n = 2$). Values are the mean ± SD.

3.3. Anti-proliferation activity of Tf-G-TPZ combined with cisplatin

The combined anti-proliferation effect of Tf-G-TPZ and cisplatin was evaluated by a cell viability assay using MTT. A serial concentration of TPZ (50–400 μM) and Tf-G-TPZ (12.5–100 μM) were selected to calculate the IC_{50} in the presence of cisplatin (20 μM) (Fig. 4). The IC_{50} of TPZ combined with cisplatin was 139.7 ± 12.1 μM. While the IC_{50} was decreased to 25.7 ± 4.2 μM

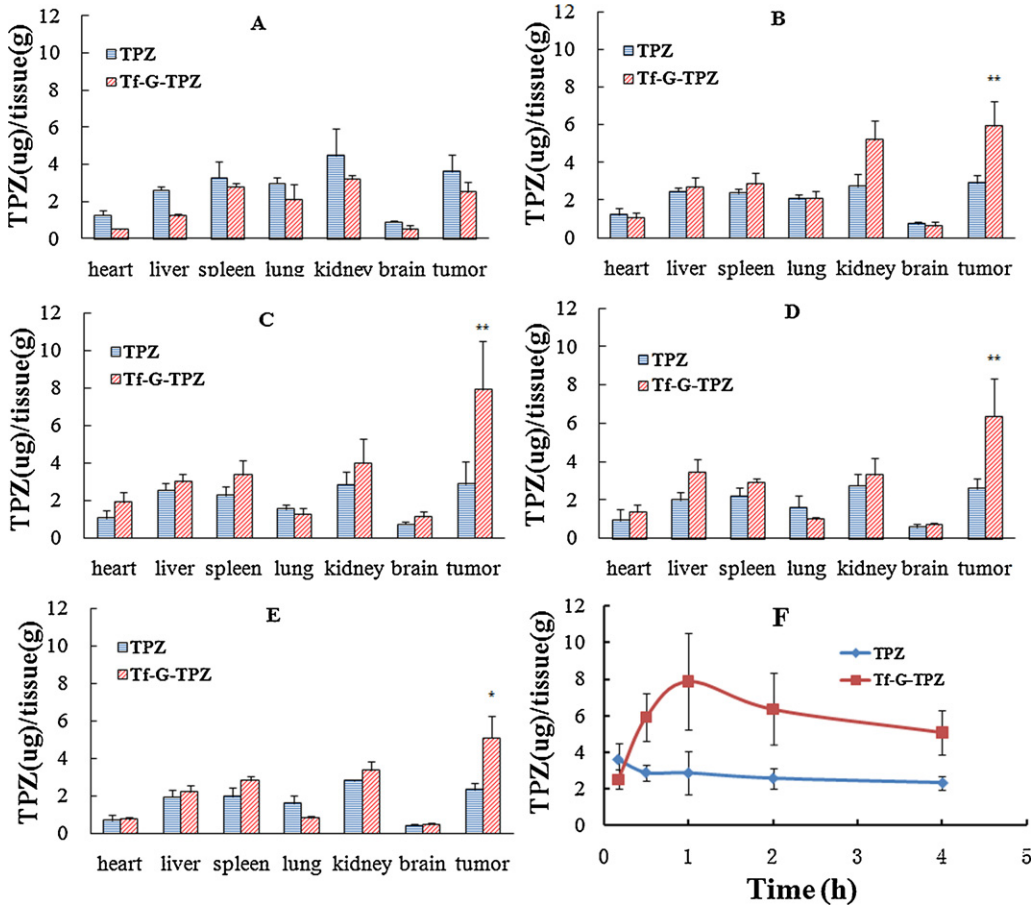

Fig. 5. Tissue distributions of TPZ and Tf-G-TPZ in S180 bearing mice. At 10 min (A), 30 min (B), 1 h (C), 2 h (D) and 4 h (E) after intravenous administration of free TPZ (20 mg/kg) or Tf-G-TPZ conjugate (containing same dose of TPZ), mice were sacrificed and the level of TPZ in different tissues were evaluated. At 30 min, 1 h, 2 h and 4 h, the level of TPZ in tumor was significantly lower than Tf-G-TPZ ($p < 0.01$). (F) Kinetics of TPZ distribution in tumor after administration as TPZ and Tf-G-TPZ. Values are the mean ± SD ($n = 4$).

when TF-G-TPZ was combined with cisplatin, indicating a significant increase in cytotoxicity. Since transferrin receptors were over-expressed on the SW1116 cell surface (Daniels et al., 2006), the cellular uptake of Tf-G-TPZ might be enhanced via transferrin receptor mediated endocytosis. Then the synergistic effect of Tf-G-TPZ and cisplatin was strengthened.

3.4. Biodistribution in S180 tumor bearing mice

To evaluate the targeting efficiency of the conjugate, TPZ and Tf-G-TPZ were intravenously injected to S180 tumor bearing mice at the dose of 20 mg/kg. Mice were sacrificed at 10 min, 30 min, 1 h, 2 h and 4 h, respectively post injection and tissues were collected to determine the level of TPZ. At 10 min post injection (Fig. 5A), TPZ was rapidly distributed to heart, liver, spleen, lung, kidney and tumor. No difference was observed between reticuloendothelial system (RES) (liver and spleen) and non-RES organs, suggesting RES were not involved in the distribution process. The concentration of TPZ in tumor was comparable to other tissues, indicating poor tumor targeting of TPZ.

Similar to TPZ, Tf-G-TPZ also rapidly distributed into heart, liver, spleen, lung, kidney and tumor after intravenous injection. At 10 min post injection, the distribution pattern of Tf-G-TPZ was almost same as TPZ (Fig. 5A). The concentration of Tf-G-TPZ was comparable to TPZ with no significant difference in tissue distribution. In contrast, at 30 min post injection, the concentration of Tf-G-TPZ in tumor was starting to increase and significantly higher than TPZ (Fig. 5B). The possible reason is due to the dimensional difference between unconjugated TPZ and conjugated TPZ. After injection, both unconjugated and conjugated TPZ distribute to tumor. Meanwhile, the distribution from tumor to blood vessel also exists. However, since the conjugated TPZ is larger than unconjugated TPZ, conjugated TPZ is more difficult to distribute to blood vessel. Therefore, at 30 min post injection the concentration of conjugated TPZ is a little bit higher than that of unconjugated TPZ. From 1 h to 4 h post injection, the concentration of Tf-G-TPZ in tumor was found to be the highest compared to all other tissues, demonstrating the targeting capacity of Tf-G-TPZ achieved through transferrin receptor-mediated endocytosis.

In tumor tissue, the pharmacokinetics of Tf-G-TPZ was significantly different from TPZ (Fig. 5F). After injection, TPZ immediately reached the maximal concentration (3.62 μg/g) and after 4 h the concentration decreased to 2.33 μg/g. While Tf-G-TPZ showed a two-phase clearance profile. At 10 min post injection, the concentration of Tf-G-TPZ in tumor tissue was only 2.52 μg/g, which was lower than TPZ. After 30 min, Tf-G-TPZ concentration kept increasing and reached the maximal concentration at 1 h (7.89 μg/g). Then the concentration started to decrease and finally reached 5.09 μg/g at 4 h post injection. Compared with TPZ, the pharmacokinetics of Tf-G-TPZ showed a delayed profile. When calculated the AUC (area under the curve) by trapezoid planimetry, the AUC of Tf-G-TPZ (46.6 μg h/g) was 2.3 fold higher than TPZ (20.1 μg h/g).

3.5. Anti-tumor efficacy and toxicity of Tf-G-TPZ combined with cisplatin

The combined anti-tumor effectiveness of Tf-G-TPZ and cisplatin was evaluated in S-180 tumor bearing mice. S180 is murine carcinoma and its growth speed is much faster than human tumor cell line (Wu et al., 2010; Xiao et al., 2004). When the tumor diameter reached about 0.5 cm, treatments including TPZ, Tf-G-TPZ, cisplatin plus TPZ and cisplatin plus Tf-G-TPZ were initiated. At 8th day post administration, the tumor size of non-treated control group was $1.5 \pm 0.3\ cm^3$, which was larger than all treatment groups (Fig. 6A). After receiving TPZ or Tf-G-TPZ, the tumor size was $1.2 \pm 0.3\ cm^3$ and $1.1 \pm 0.2\ cm^3$, respectively. Compared with

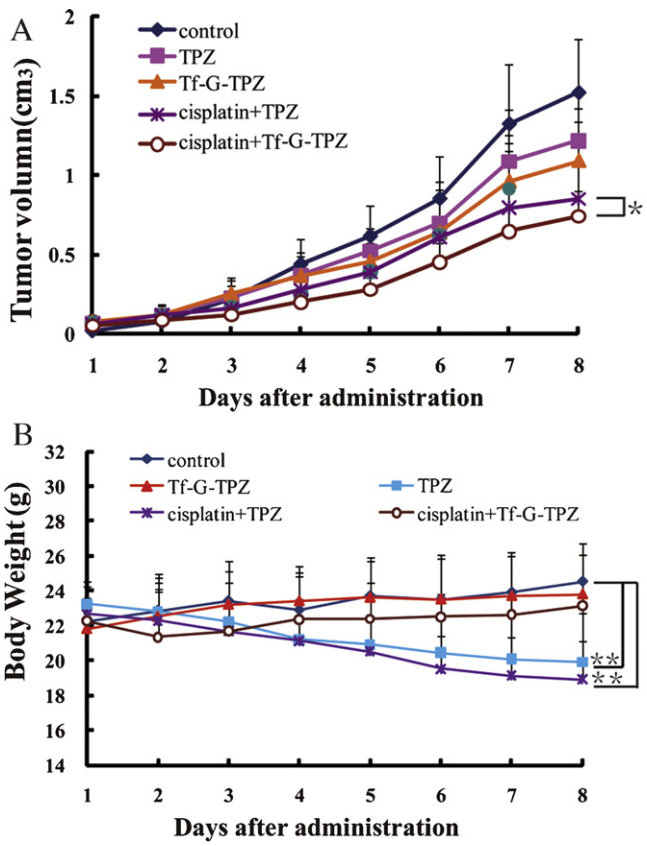

Fig. 6. Anti-tumor effects in treated mice. (A) Administrations were carried out daily with an eight-day interval into S180 tumor bearing mice. Tumor volume was monitored daily. Tf-G-TPZ plus cisplatin resulted in significant retardation of tumor growth, compared to the treatments of only Tf-G-TPZ or combination of TPZ/cisplatin ($p < 0.05$). (B) Weight changes of treated mice with S180 solid tumors. A significant weight loss was observed in groups treated with cisplatin, TPZ and TPZ plus cisplatin. While groups treated with Tf-G-TPZ and Tf-G-TPZ plus cisplatin showed a slight change in the body weight after 8 days ($n = 9$ or 10, $^*p < 0.05$, $^{**}p < 0.01$).

the control group, the tumor inhibition of TPZ and Tf-G-TPZ was 20% and 26%, respectively. To achieve better tumor inhibition, TPZ was co-administered with cisplatin. After 8 days' treatment, the tumor size was around $0.9\ cm^3$, which was smaller than all the above treatment groups. The synergistic effects of TPZ and cisplatin might be partially due to their different mechanisms for tumor inhibition. Cisplatin could inhibit the formation of DNA intrastrand and interstrand adducts (Rischin et al., 2001) while TPZ could inhibit the repair of cisplatin-induced interstrand adducts (Kovacs et al., 1999).

Since transferrin could target anti-tumor drugs to tumor and increase the tumor inhibition, TPZ was conjugated with transferrin and co-administered with cisplatin for enhanced antitumor efficacy. Results showed that when Tf-G-TPZ was combined with cisplatin, the tumor size was reduced to only $0.7 \pm 0.2\ cm^3$. Compared with the control group, the tumor inhibition reached 53%, which achieved the highest tumor inhibition among all treatment groups. The enhanced antitumor effects of combination therapy might arise from the high distribution in tumor tissue as shown in Fig. 5. Upon conjugated with transferrin, TPZ could be accumulated in tumor tissue since the transferrin receptor was overexpressed on the tumor cell surface. The extended residence of Tf-G-TPZ in tumor might result in an increased synergistic effect with cisplatin and thus an enhanced antitumor efficacy was achieved.

Despite of the antitumor efficacy, a significant weight loss of the modeled animal was observed in groups treated with cisplatin,

TPZ and TPZ plus cisplatin. Notably, the body weight (18.9 ± 2.2 g) treated with TPZ plus cisplatin was the lowest among all treatment groups, suggesting the side effects of the combination therapy. In contrast, the body weight was almost constant in the group treated with Tf-G-TPZ, regardless of combination with cisplatin or not (Fig. 5B). The slight changes of weight in the group treated with Tf-G-TPZ might be due to the targeted delivery of TPZ via transferrin. Only after Tf-G-TPZ was transferred into tumor cell, can TPZ be released to perform antitumor activity. In normal tissue with low expression of transferrin, the concentration of TPZ could be much lower than in tumor, thus resulting in low synergistic effects.

4. Conclusions

The combination of TPZ with cisplatin has been extensively studied in clinical trial for tumor therapy. However, in phase III clinical trial, the combinatorial therapy did not show overall improvement in patients with advanced head and neck cancer. To increase the efficacy and reduce the side effects of the combination therapy, TPZ was conjugated with transferrin for targeted delivery to tumor cells, since transferrin receptors were overexpressed on tumor cells. Results from this study suggest that the conjugate could enrich TPZ and increase its residence time in tumor tissue. Due to the enhanced exposure of TPZ to tumor, the synergistic effects when co-administered with cisplatin were also increased. Therefore, Tf-G-TPZ shows great promise as substitute for TPZ in the combined therapy with cisplatin.

Acknowledgments

This paper was supported by the Fundamental Research Funds for the Central Universities (Nos. 1107020836 and 1118020806), Research Fund for the Doctoral Program of Higher Education of China (No. 20110091120044), Natural Science Foundation of Jiangsu (Nos. BK2011572 and BK2011539), National Natural Science Foundation (No. 30973651), Science & Technology Support Program of Jiangsu Province (No. BE2010719) and Changzhou Special Project of Biotechnology and Biopharmacy (No. CE20105006).

References

Abuzeid, W.M., Jiang, X., Shi, G., Wang, H., Paulson, D., Araki, K., Jungreis, D., Carney, J., O'Malley Jr., B.W., Li, D., 2009. Molecular disruption of RAD50 sensitizes human tumor cells to cisplatin-based chemotherapy. J. Clin. Invest. 119, 1974–1985.

Adam, M., Ottenjann, S., Kunzel, G., Busch, R., Erhardt, W., Nieder, C., Molls, M., 2006. Evaluation of the toxicity of tirapazamine plus cisplatin in a mouse tumor model. Strahlenther. Onkol., 231–239.

Amet, N., Wang, W., Shen, W.C., 2010. Human growth hormone–transferrin fusion protein for oral delivery in hypophysectomized rats. J. Control. Release 141, 177–182.

Beyer, U., Roth, T., Schumacher, P., Maier, G., Unold, A., Frahm, A.W., Fiebig, H.H., Unger, C., Kratz, F., 1998. Synthesis and in vitro efficacy of transferrin conjugates of the anticancer drug chlorambucil. J. Med. Chem. 41, 2701–2708.

Covens, A., Blessing, J., Bender, D., Mannel, R., Morgan, M., 2006. A phase II evaluation of tirapazamine plus cisplatin in the treatment of recurrent platinum-sensitive ovarian or primary peritoneal cancer: a Gynecologic Oncology Group study. Gynecol. Oncol. 100, 586–590.

Crul, M., van Waardenburg, R.C., Beijnen, J.H., Schellens, J.H., 2002. DNA-based drug interactions of cisplatin. Cancer Treat. Rev. 28, 291–303.

Daniels, T.R., Delgado, T., Helguera, G., Penichet, M.L., 2006. The transferrin receptor. Part II. Targeted delivery of therapeutic agents into cancer cells. Clin. Immunol. 121, 159–176.

Dickson, M.A., Carvajal, R.D., Merrill Jr., A.H., Gonen, M., Cane, L.M., Schwartz, G.K., 2011. A phase I clinical trial of safingol in combination with cisplatin in advanced solid tumors. Clin. Cancer Res. 17, 2484–2492.

Fruscio, R., Garbi, A., Parma, G., Lissoni, A.A., Garavaglia, D., Bonazzi, C.M., Dell'anna, T., Mangioni, C., Milani, R., Colombo, N., 2011. Randomized phase III clinical trial evaluating weekly cisplatin for advanced epithelial ovarian cancer. J. Natl. Cancer Inst. 103, 347–351.

Hong, M., Zhu, S., Jiang, Y., Tang, G., Sun, C., Fang, C., Shi, B., Pei, Y., 2010. Novel anti-tumor strategy: PEG–hydroxycamptothecin conjugate loaded transferrin–PEG-nanoparticles. J. Control. Release 141, 22–29.

Jensen, M.P., Gorman-Lewis, D., Aryal, B., Paunesku, T., Vogt, S., Rickert, P.G., Seifert, S., Lai, B., Woloschak, G.E., Soderholm, L., 2011. An iron-dependent and transferrin-mediated cellular uptake pathway for plutonium. Nat. Chem. Biol. 7, 560–565.

Kato, Y., Tsukada, Y., Hara, T., Hirai, H., 1983. Enhanced antitumor activity of mitomycin C conjugated with anti-alpha-fetoprotein antibody by a novel method of conjugation. J. Appl. Biochem. 5, 313–319.

Koberle, B., Tomicic, M.T., Usanova, S., Kaina, B., 2010. Cisplatin resistance: preclinical findings and clinical implications. Biochim. Biophys. Acta 1806, 172–182.

Kovacs, M.S., Hocking, D.J., Evans, J.W., Siim, B.G., Wouters, B.G., Brown, J.M., 1999. Cisplatin anti-tumour potentiation by tirapazamine results from a hypoxia-dependent cellular sensitization to cisplatin. Br. J. Cancer 80, 1245–1251.

Kratz, F., Beyer, U., Roth, T., Tarasova, N., Collery, P., Lechenault, F., Cazabat, A., Schumacher, P., Unger, C., Falken, U., 1998. Transferrin conjugates of doxorubicin: synthesis, characterization, cellular uptake, and in vitro efficacy. J. Pharm. Sci. 87, 338–346.

Liu, Y., Shen, B., Liu, F., Zhang, B., Chu, T., Bai, J., Bao, S., 2012. Synthesis, radiolabeling, biodistribution and fluorescent imaging of histidine-coupled hematoporphyrin. Nucl. Med. Biol., http://dx.doi.org/10.1016/j.nucmedbio.2011.10.010.

Marcu, L., Olver, I., 2006. Tirapazamine: from bench to clinical trials. Curr. Clin. Pharmacol. 1, 71–79.

Moriyama-Gonda, N., Shiina, H., Terashima, M., Satoh, K., Igawa, M., 2008. Rationale and clinical implication of combined chemotherapy with cisplatin and oestrogen in prostate cancer: primary evidence based on methylation analysis of oestrogen receptor-alpha. BJU Int. 101, 485–491.

Ofner 3rd, C.M., Pica, K., Bowman, B.J., Chen, C.S., 2006. Growth inhibition, drug load, and degradation studies of gelatin/methotrexate conjugates. Int. J. Pharm. 308, 90–99.

Park, K., 2010. Tumor regression after systemic administration of transferrin-targeted TNFalpha plasmid–dendrimer conjugates. J. Control. Release 143, 167.

Qin, C., Du, Y., Xiao, L., Li, Z., Gao, X., 2002. Enzymic preparation of water-soluble chitosan and their antitumor activity. Int. J. Biol. Macromol. 31, 111–117.

Rainov, N.G., Soling, A., 2006. Clinical studies with targeted toxins in malignant glioma. Rev. Recent Clin. Trials 1, 119–131.

Reddy, S.B., Williamson, S.K., 2009. Tirapazamine: a novel agent targeting hypoxic tumor cells. Expert Opin. Investig. Drugs 18, 77–87.

Rischin, D., Peters, L., Hicks, R., Hughes, P., Fisher, R., Hart, R., Sexton, M., D'Costa, I., von Roemeling, R., 2001. Phase I trial of concurrent tirapazamine, cisplatin, and radiotherapy in patients with advanced head and neck cancer. J. Clin. Oncol. 19, 535–542.

Rischin, D., Peters, L.J., O'Sullivan, B., Giralt, J., Fisher, R., Yuen, K., Trotti, A., Bernier, J., Bourhis, J., Ringash, J., Henke, M., Kenny, L., 2010. Tirapazamine, cisplatin, and radiation versus cisplatin and radiation for advanced squamous cell carcinoma of the head and neck (TROG 02.02. HeadSTART): a phase III trial of the Trans-Tasman Radiation Oncology Group. J. Clin. Oncol. 28, 2989–2995.

Rosenberg, B., Vancamp, L., Krigas, T., 1965. Inhibition of cell division in *Escherichia coli* by electrolysis products from a platinum electrode. Nature 205, 698–699.

Siim, B.G., Pruijn, F.B., Sturman, J.R., Hogg, A., Hay, M.P., Brown, J.M., Wilson, W.R., 2004. Selective potentiation of the hypoxic cytotoxicity of tirapazamine by its 1-N-oxide metabolite SR 4317. Cancer Res. 64, 736–742.

Stordal, B., Davey, M., 2007. Understanding cisplatin resistance using cellular models. IUBMB Life 59, 696–699.

Tikoo, K., Kumar, P., Gupta, J., 2009. Rosiglitazone synergizes anticancer activity of cisplatin and reduces its nephrotoxicity in 7,12-dimethyl benz{a}anthracene (DMBA) induced breast cancer rats. BMC Cancer 9, 107.

Todd, R.C., Lippard, S.J., 2009. Inhibition of transcription by platinum antitumor compounds. Metallomics 1, 280–291.

Wang, Y., Chen, Y.S., Zaro, J.L., Shen, W.C., 2011. Receptor-mediated activation of a proinsulin–transferrin fusion protein in hepatoma cells. J. Control Release, http://dx.doi.org/10.1016/j.jconrel.2011.06.029.

Wu, D., Gao, Y., Chen, L., Qi, Y., Kang, Q., Wang, H., Zhu, L., Ye, Y., Zhai, M., 2010. Antitumor effects of a novel chimeric peptide on S180 and H22 xenografts bearing nude mice. Peptides 31, 850–864.

Wu, J., Ding, D., Ren, G., Xu, X., Yin, X., Hu, Y., 2009. Sustained delivery of endostatin improves the efficacy of therapy in Lewis lung cancer model. J. Control. Release 134, 91–97.

Wu, L., Wu, J., Zhang, J., Zhou, Y., Ren, G., Hu, Y., 2008. A simple method for obtaining transferrins from human plasma and porcine serum: preparations and properties. J. Chromatogr. B 867, 62–68.

Xiao, C., Qi, X., Maitani, Y., Nagai, T., 2004. Sustained release of cisplatin from multivesicular liposomes: potentiation of antitumor efficacy against S180 murine carcinoma. J. Pharm. Sci. 93, 1718–1724.

Yamasaki, M., Miyata, H., Tanaka, K., Shiraishi, O., Motoori, M., Peng, Y.F., Yasuda, T., Yano, M., Shiozaki, H., Mori, M., Doki, Y., 2011. Multicenter phase I/II study of docetaxel, cisplatin and fluorouracil combination chemotherapy in patients with advanced or recurrent squamous cell carcinoma of the esophagus. Oncology 80, 307–313.

Ying, X., Li-Zhi, L., Li-Ping, C., Min, Z., Ji-Hong, L., 2011. Clinical effects of irinotecan hydrochloride in combination with cisplatin as neoadjuvant chemotherapy in locally advanced cervical cancer. Gynecol. Oncol., 99–104.